

Microwave Absorption Properties of Polyaniline/Poly(vinyl alcohol)/Multi-Walled Carbon Nanotube Composites in Thin Film and Nanofiber Layer Structures

Golestan Salimbeygi, Komeil Nasouri, Ahmad Mousavi Shoushtari*, Reza Malek, and Firoozmehr Mazaheri

Department of Textile Engineering, AmirKabir University of Technology, Tehran 15875-4413, Iran.

Received February 10, 2015; Revised April 16, 2015; Accepted June 1, 2015

Abstract: Electrospinning of conductive polymer blends offers high potential to prepare novel materials for electrical applications. The main aim of this work is to fabricate poly(vinyl alcohol) (PVA), polyaniline (PANI), and multi walled carbon nanotubes (MWNT) composites in thin film and nanofiber layer structures and then compare their microwave absorption behavior. First, optimum ratios for blending PVA, PANI, Camphorsulfonic acid (CSA) and MWNT were obtained. Then under optimized ratios, composite solutions of PVA: PANI-CSA, and PVA/PANI-CSA/MWNT were fabricated to nanofiber layer and thin film structures. Based on scanning electron microscope (SEM) micrographs, the PVA/PANI-CSA nanofiber samples at low content of PANI-CSA presented a very uniform surface and without any beads but some beads started to develop at higher PANI-CSA content. However, the SEM analysis of the PVA/PANI-CSA/MWNT films revealed the uniform appearance for all composites. But, some aggregation and local irregularities on the surface were observed due to the presence of MWNT in the composite structure. Microwave absorption behavior was evaluated using vector network analyzers in the frequency range of 8-12 GHz (X-band) for all samples. It was observed that absorption microwave properties of PVA/PANI-CSA nanofibers improved with increasing in the loading levels of PANI-CSA in the mixture. Microwave absorption properties of the PVA/PANI-CSA/MWNT composite nanofiber absorbers have been compared with thin films at various thicknesses by measuring the relative maximum reflection loss (dB/mm) of samples. The PVA/PANI-CSA/MWNT composite nanofibers with the layer thickness of 0.1 mm presented two remarkable absorbing peaks versus one absorbing peak in nanocomposite films with similar thickness. The relative maximum reflection loss in PVA/PANI-CSA/MWNT composite nanofiber has reached -230 dB/mm at frequency of 8.6 GHz which is nearly 8 times higher than -28 dB/mm at frequency of 8.4 GHz for PVA/PANI-CSA/MWNT film samples.

Keywords: carbon nanotubes, polyaniline, composite nanofiber, nanocomposite film, microwave absorption.

Introduction

In recent years, electromagnetic pollution has increased by the rising prevalence of electrical and electronic devices and it has become a serious concern in modern societies. Electromagnetic interference (EMI) can cause serious problems including not only loss of time, energy, resources, money but also increase of human morbidity and mortality.^{1,2} Some kinds of shielding mechanisms have been proposed, namely: surface reflection, absorption and multiple reflections. Nowadays, high performance electromagnetic absorption materials (EMAs) have been extensively investigated for anti-electromagnetic interference coatings, microwave darkroom and their potential application in stealth technology and military purposes.³⁻⁵

The electromagnetic absorbing performance of any materials depends on intrinsic electromagnetic and extrinsic properties. The intrinsic electromagnetic properties include conductivity,

complex permittivity and permeability. The extrinsic properties consist of thickness, working frequency, morphology and material structure.^{6,7} Inorganic materials such as ferrites and metal powders possess large electric and magnetic loss and usually are used as electromagnetic wave absorbers⁷ but some disadvantages such as high density, poor environmental stability and processability have restricted their wide applications as electromagnetic wave absorber.⁸ On the contrary, polymer composite materials possess low densities, easy processability and high electromagnetic properties. The polymeric substances could overcome the restriction mentioned above.⁷ However to achieve desired electromagnetic performance from fabricated absorber, both of electric and magnetic component of the electromagnetic wave needs to be absorbed and therefore the dielectric or magnetic fillers are usually added to the polymer matrix.⁹ Instead of applying regular polymeric substance added by some metallic powder using intrinsically conducting polymers (ICPs) that are known as "synthetic metals"¹⁰ can be a good alternative since ICPs

*Corresponding Author. E-mail: amousavi@aut.ac.ir

have processability and electrical properties, simultaneously.¹¹ Therefore, EMI shielding/absorbing has been considered as one of its potential applications.¹² Among the ICPs, polyaniline (PANI) has attracted more attention because of its unique non-redox doping, excellent thermal, chemical and environmental stability, processability and tunable properties compared to other conducting polymers.^{13,14} Many researchers have studied on the electromagnetic shielding behavior of PANI and its related composites.¹⁵⁻¹⁷ Electrical conductivity and presence of bound/localized charges can supply strong polarization and relaxation effect leading to high dielectric loss in PANI structures.^{11,18} On the other hand, the magnetic (H-field) component of electromagnetic energy can be absorbed by material that possesses magnetic properties. Multi-wall carbon nanotubes (MWNT) with moderate magnetization (M_s) can be a potential candidate for this purpose.¹⁹ Moreover, carbon nanotubes are known to possess exceptional mechanical, electrical and thermal properties, excellent electrical conductivities and high aspect ratio²⁰⁻²³ that have made them very promising for high-tech applications.^{24,25} By combining the good properties of MWNT and PANI and incorporation of a magnetic filler and dielectric matrix, the PANI/MWNT composites may possess synergetic effects. Therefore, it is expected to achieve higher absorption of electromagnetic energy by this kind of microwave absorbing material. However, due to the poor mechanical properties of PANI as an intrinsically conducting polymer, it is necessary to blend it with a matrix based on polymeric systems for any commercially useful product.

The present study aims to investigate the electromagnetic wave absorption behavior of PVA/PANI/MWNT composites in electrospun nanofibers and nanocomposite film. Nanostructure materials with larger specific surface area, more number of surface active atoms leading to larger interface dielectric and magnetic loss.⁷ Because of their good dielectric and/or magnetic loss, nanostructure materials are most promising material to improve the electromagnetic wave absorption property. Recently, though nanocomposites have extensively been studied as EMI shielding/absorbing materials but only few brief reports are available on the EMI shielding properties and specially microwave absorption characteristics for nanofiber structure.^{4,26} In this study, PVA/PANI electrospun nanofibers with different proportion of polyaniline in the blend were prepared and then, PVA/PANI/MWNT composites in electrospun nanofibers and nanocomposite film forms were fabricated and finally their microwave absorption behaviors were compared at X-band microwave frequencies.

Experimental

Materials. PVA powder ($M_w=72,000$ g/mol, 98% hydrolyzed) as a matrix was obtained from Merck. Distilled water was used as the solvent of PVA. PANI powder (emeraldine base, $M_w=100,000$ g/mol) as a polymer, camphorsul-

fonic acid (CSA) as a PANI doping agent, and *N*-methyl-2-pyrrolidone (NMP) as a PANI solvent were obtained from Sigma-Aldrich. MWNT (purity>95%, diameter<8 nm, Length: 30 μm) were purchased from Neutrino Company. Sodium dodecyl sulfate (SDS) as a dispersing agent was obtained from Merck. Glutaraldehyde (GA, grade I) and sulfuric acid (H_2SO_4 , purity>99.999%) for crosslinking of PVA were obtained from Aldrich Company. All used reagents were of analytical grade and were used as received without further purification.

Preparation of PVA/PANI-CSA Solutions. The main steps of PVA/PANI-CSA solutions preparation are shown in Figure 1. The PANI-CSA solutions were prepared in two steps. First, 10,000 mg of high-molecular weight emeraldine base PANI was dissolved in 100 mL of NMP by using a magnetic stirrer (corning hot plate stirrer PC-351) at 25 °C for 2 h. In the second step, 10,000 mg of CSA was added for doping of PANI a magnetic stirrer at 25 °C for 1 h was used to give a PANI: CSA ratio of 1:1. The PVA solution was also prepared by dissolving 8 wt% of PVA in distill water by using a magnetic stirrer at 80 °C for 2 h. Finally, the PVA and PANI-CSA solutions were mixed to obtain a 1:0, 1:1, and 1:2 PVA/PANI-CSA ratio.

Preparation of PVA/PANI-CSA/MWNT Composite Solutions. The main steps of PVA/PANI-CSA/MWNT composite solutions preparation are shown in Figure 2. Preparing well dispersed MWNT solutions due to their strong van der Waals interactions is difficult. To prepare dispersed MWNT in distilled water uniformly, SDS surfactant applied. The SDS/ H_2O solution was prepared by dissolving 1 wt% SDS in distilled water using a magnetic stirrer at 25 °C for 1 h. Then, different weights of MWNT were dispersed in the SDS/ H_2O solutions by using a high power ultrasonic homogenizer (UP200, Germany) at 0 °C for 20 min. The PVA/MWNT/SDS solutions were prepared by dissolving 10 wt% of PVA in sonicated solutions by using a magnetic stirrer at 80 °C for 2 h. Finally, preparing of PVA/PANI-CSA/MWNT solutions were carried out by mixing PVA/MWNT/SDS and PANI-CSA solutions by considering a PVA: PANI-CSA::1:2 ratio.

Nanofiber Layers Fabrication. The prepared PVA/PANI-

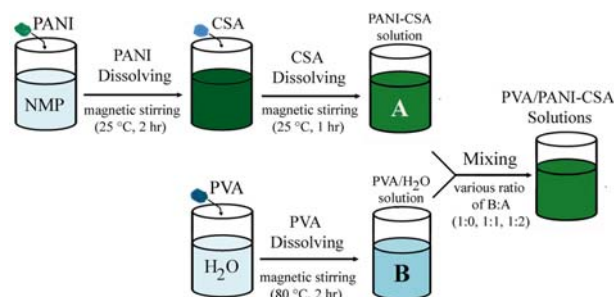


Figure 1. Illustration of PVA/PANI-CSA solutions preparation steps.

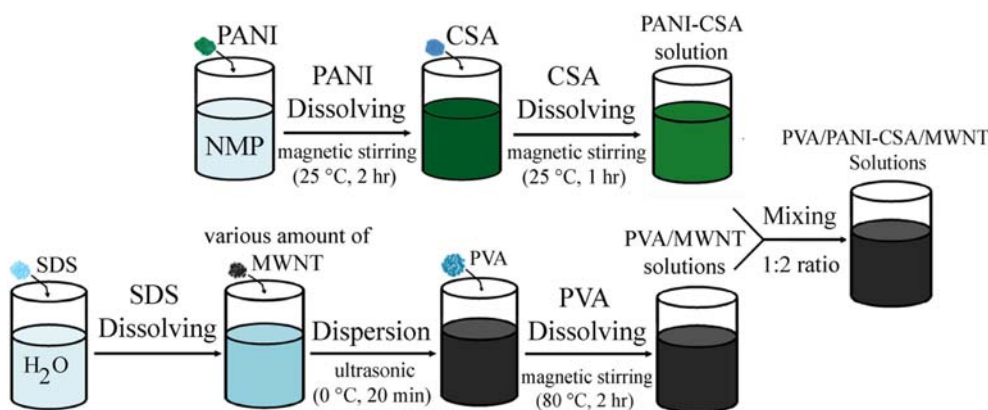


Figure 2. Illustration of PVA/PANI-CSA/MWNT solutions preparation steps.

CSA and PVA/PANI-CSA/MWNT composite solutions were added to a glass syringe with a needle tip (22G, L=34 mm, O.D=0.7 mm, and I.D=0.4 mm). The feeding rate of the polymer solutions was set to 0.25 mL/h, electrospinning voltage of 15 kV was applied to the needle, the distance between the needle tip and collector ($D=8.15$ cm) was 17 cm and collector speed of 100 rpm was set for collecting the electrospun nanofiber layers. The electrospinning of all solutions were performed at 22 ± 2 °C and constant relative humidity of 35–40%. The thickness of the fabricated nanofiber samples was set on 100 μm .

Preparation of PVA/PANI/MWNT Thin Film. The prepared PVA/PANI-CSA/MWNT composite solutions were cast onto a stainless steel mold and dried at 40 °C for 24 h. Finally, the films were removed from the molds and stored in desiccators prior to use. The thicknesses of the fabricated films were set on 1 mm.

Cross Linking Treatment. The resulting films and nanofiber layers were kept in desiccators at room temperature for 24 h, and then were cross-linked by using 0.01 wt% GA and 0.5 wt% H_2SO_4 as a catalyst for 1 h. The final films and nanofibers were obtained after washing with distilled water. The PVA/PANI-CSA/MWNT cross-linked films and nanofibers products were designated as PANIMWNT-0 (0 wt% MWNT), PANIMWNT-2 (2 wt% MWNT), PANIMWNT-5 (5 wt% MWNT), and PANIMWNT-10 (10 wt% MWNT).

Measurement and Characterization. The surface morphology of the nanofiber layers and film composites was examined by SEM (Philips, XL-30) at an accelerating voltage of 25 kV under magnification of 5000 \times and 10000 \times . The average fiber diameter was measured with the SEM images using Image J software (National Institute of Health, USA) from 100 fibers. The microwave-absorbing properties of all samples were investigated by HP Vector Network Analyzer (Model 8510ES) in the frequency range of 8–12 GHz at room temperature. All samples were cut into a rectangular shape (22.86 mm \times 10.16 mm) to fit in rectangular wave-guide of X-band.

Results and Discussion

Morphology of PVA/PANI-CSA Nanofibers. Figure 3 displays SEM photographs and corresponding fiber diameter distribution of PVA/PANI-CSA nanofiber samples prepared under PVA: PANI ratios of 1:0, 1:1, and 1:2. As it can be seen in Figure 3(a), the surface of the electrospun nanofibers is very smooth and uniform. It was observed that small beads have been formed, when the PANI content was increased (see the sample ratio PVA: PANI of 1:1 in Figure 3(b)), and become

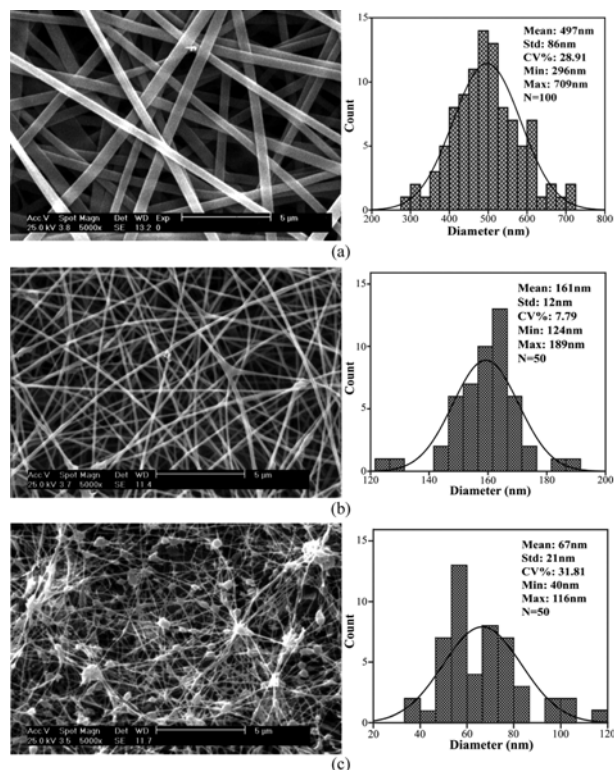


Figure 3. SEM photographs (left) and corresponding fibers diameter distribution (right) of electrospun nanofibers samples with PVA:PANI ratios of (a) 1:0, (b) 1:1, and (c) 1:2

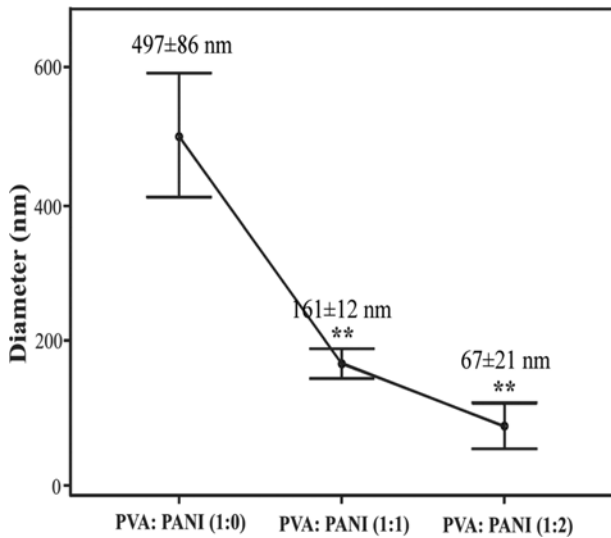


Figure 4. Error plot of nanofibers average diameter versus PANI loading (*: $p < 0.05$, values are significantly different from the previous group compared).

larger and more at higher PANI content for PVA:PANI sample with a ratio of 1:2 in Figure 3(c). As described in the literature,²⁷ the viscosity of the solution is significantly decreased with increasing of PANI content and consequently bead formation can be still observed at higher PANI ratios during the electrospinning process.^{28,29}

Changes in the average diameter of the various produced nanofiber samples with increasing the PANI concentration are shown in Figure 4. The diameter of the fabricated nanofibers decreased rapidly with increasing in PANI concentration. The diameter of PVA/PANI nanofibers kept decreasing gradually with further increasing in PANI concentration. With increasing the PANI loading in the mixture from 0 to 50%, the mean diameter of nanofibers decreased from 497 ± 86 to 161 ± 21 nm. Moreover, when the PANI loading in the mixture was increased to 75% the average diameter decreased to 67 ± 21 nm. The average nanofibers diameter of the all samples were significantly different from previous groups. Low viscosity of the solution causes a low viscoelastic force and due to coulombic repulsion. The lower viscoelastic force versus the higher electrostatic force can lead to decrease in the average diameter of nanofibers.^{26,30} On the other hand, this reduction in diameter results from the enhanced conductivity of the polymer solution with increasing in PANI content. Large electric current produced during electrospinning causes large charge accumulation in the solution jet and therefore strong electrostatic repulsion could be produced. Thus the repulsive force can overcome the surface tension of the jet and leading to a remarkable reduction in nanofibers diameter.³¹

Electromagnetic Properties of the PVA/PANI-CSA Nanofibers. The electromagnetic absorbing properties of the absorbers can be defined by the reflection loss. The reflection loss

(RL) is described as:

$$RL = 20 \log_{10} \left| \frac{Z_{in} - Z_0}{Z_{in} + Z_0} \right| \quad (1)$$

where Z_{in} is the input impedance at the air-material interface and Z_0 is the intrinsic impedance of free space and are calculated as follows:

$$Z_{in} = \sqrt{\frac{\mu_0 \mu}{\epsilon_0 \epsilon}} \tanh(j2\pi f d \sqrt{\mu \mu_0 \epsilon \epsilon_0}) \quad (2)$$

$$Z_0 = \sqrt{\frac{\mu_0}{\epsilon_0}} = 120 \pi \quad (3)$$

In these equations, μ_0 and ϵ_0 are the complex permeability and complex permittivity of free space, μ and ϵ are the complex permeability and permittivity respectively, d is the material's thickness and f is the frequency of the electromagnetic wave.³²

In order to investigate the microwave absorption property of the prepared samples, the reflection loss was measured at the range of 8-12 GHz. Microwave absorption property in X-band frequency range of 8.2-12.4 GHz is more important for many electrical and commercial applications, such as in Doppler, weather radar, Satellite Radiolocation, Maritime Radio-navigation, TV picture transmission, and telephone microwave relay systems. The frequency dependencies of the microwave absorbing properties of the PVA/PANI-CSA nanofibers samples are shown in Figure 5. For PVA/PANI (1:0) sample, the maximum reflection loss reached to -6.5 dB at frequency of 11.5 GHz. While in PVA/PANI (1:1) sample, two absorption peaks were observed, the first peak at frequency of 11.6 GHz reached to -9 dB and the second one increased to -10 dB at frequency of 11.5 GHz. However, PVA/PANI (1:2) sample presented better electromagnetic absorption properties than others in which the first maximum absorption peak was increased to -11 dB at the frequency of 8.5 GHz and the second maximum absorption peak was increased to -10 dB at the frequency of 11 GHz. This results indicate that the microwave absorbing properties have improved in higher PANI loading and conductive PANI plays a great role in

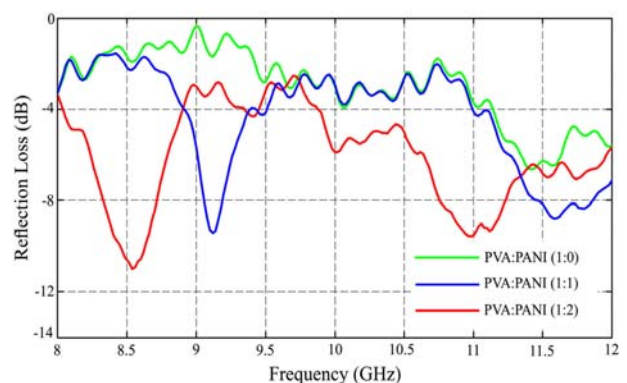


Figure 5. Reflection loss dependency on the frequency for the PVA/PANI-CSA nanofibers.

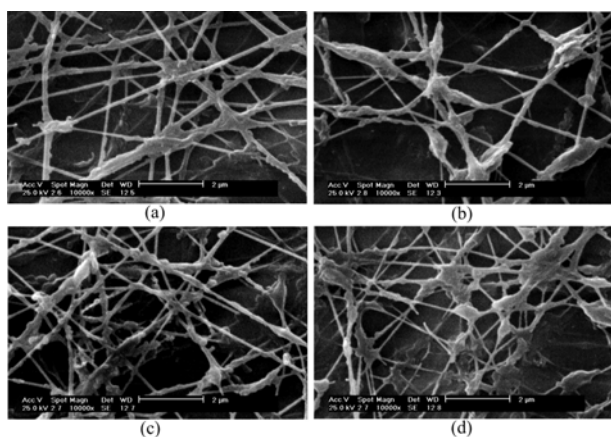


Figure 6. SEM photographs of electrospun composite nanofibers layers samples: (a) PANIMWNT-0, (b) PANIMWNT-2, (c) PANIMWNT-5, and (d) PANIMWNT-10.

improving microwave absorption.

In general, high conductivity, good dielectric permittivity and magnetic permeability lead to high electromagnetic absorption.²⁵ As described in the literature,^{29,33-35} PANI has the highest value of dielectric constant which is attributed to the disordered motion of charge carriers along the backbone of conducting PANI. In fact, the intrinsic metallic nature of conducting PANI such as conductivity and charge delocalization lead to a desired dielectric response. By considering the fact that, with increasing the PANI content, higher conductivity and dielectric properties can be achieved, therefore, in all PVA/PANI/MWNT nanofiber samples, PVA:PANI ratio of 1:2 was used.

Morphology of the PVA/PANI/MWNT Composite Nanofibers. Figure 6 shows SEM photographs of PVA/PANI-CSA/MWNT nanofibers layers. As it can be seen, low surface roughness in the composite nanofibers samples with small beads can be observed. The small beads became larger at the presence of MWNT and more by increasing the concentration of MWNT.

Electromagnetic Properties of the PVA/PANI/MWNT Composite Nanofibers. Figure 7 shows the calculated results of reflection loss versus frequency for the PVA/PANI/MWNT composite nanofibers layers. As it can be seen, all reflection loss curves presented at least two remarkable absorption peaks in the frequency range of 8-12 GHz. The first absorption peak value for the PANIMWNT-0 sample, was -11 dB at frequencies of 8.5 GHz and the second peak value was -10 dB at the frequency of 11 GHz. For the PANIMWNT-2 sample, the values of both absorption peaks have increased to -12 and -11 dB, respectively and the electromagnetic absorption properties improved about 2 dB in the 8.6-12 GHz frequency range. With increasing of MWNT concentration to 5 wt% for PANIMWNT-5 sample, the first maximum absorption peak has been observed at the frequency of 8.6 GHz and reached -11 dB, the second maximum absorption peak has

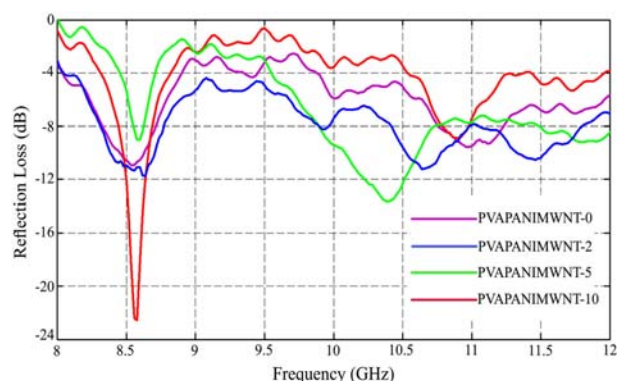


Figure 7. Reflection loss dependency on the frequency for the PVA/PANI/MWNT nanofibers.

been observed at a frequency of 10.3 GHz and has heightened to -14 dB. Finally, for the PANIMWNT-10 sample with content of 10 wt% MWNT, the second absorption peak at the frequency of 10.7 GHz has decreased to 9 dB, but the reflection loss has raised to -23 dB at the frequency of 8.6 GHz.

Morphology of the PVA/PANI/MWNT Films. The surface of the PVA/PANI/MWNT films was examined directly using a scanning electron microscope. Figure 8 displays SEM photographs the surface of cast films. Very uniform and evenness surface can be seen in Figure 8(a) for PANIMWNT-0 film. In the presence of MWNT, the surface morphology of the film completely changed. Presence of MWNT on the surface of the film can be seen in the Figure 8(b) for PANIMWNT-2 sample. When the MWNT content was increased to 5 wt% for PANIMWNT-5 sample in Figure 8(c), the surface morphology of the film changed again. Finally, in concentration 10 wt% MWNT for PANIMWNT-10 sample in Figure 8(d), some aggregation and local irregularities were observed on the sample's surface.

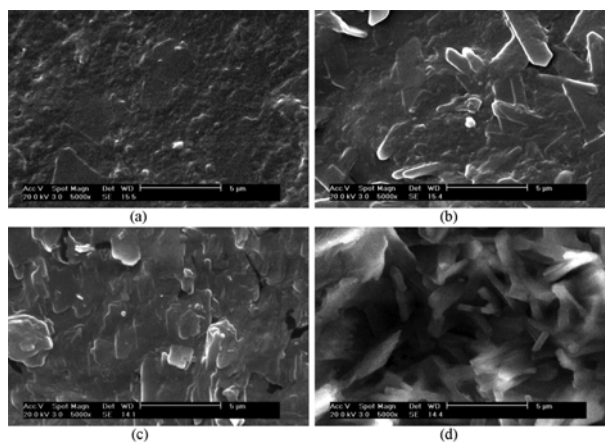


Figure 8. SEM photographs of composite film samples at magnification in SEM imaging 5000 \times : (a) PANIMWNT-0, (b) PANIMWNT-2, (c) PANIMWNT-5, and (d) PANIMWNT-10.

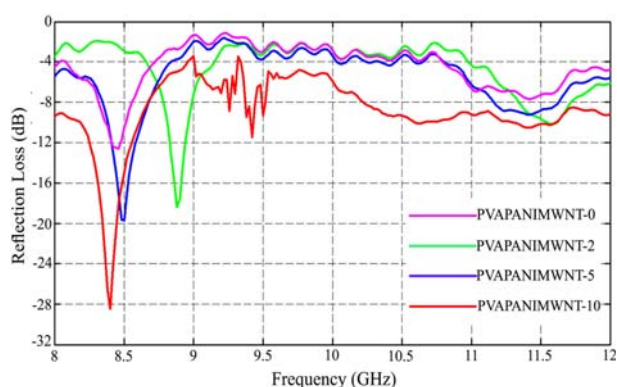


Figure 9. Reflection loss dependency on the frequency for the PVA/PANI-CSA/MWNT nanocomposite films.

Electromagnetic Properties of the PVA/PANI/MWNT Films. The variation of reflection loss versus frequency for PVA/PANI/MWNT film samples is shown in Figure 9. The results demonstrated one absorption peak for all samples in the frequency range 8–12 GHz. For PANIMWNT-0 film, the value of the absorption peak was -13 dB at a frequency of 8.4 GHz and the reflection loss value in the 8.6–12 GHz frequency range was fluctuated from 1 to 8 dB. For PANIMWNT-2, the absorption peak value increased to -17 dB at the frequency of 8.8 GHz and the maximum reflection loss enlarged to 10 dB at a frequency of 11.5 GHz. With increasing of MWNT concentration to 5 wt% for PANIMWNT-5 film, the maximum reflection loss increased to -18 dB at a frequency of 8.5 GHz. For the PANIMWNT-10 film with a maximum content of MWNT, the maximum reflection loss grew to -28 dB at the frequency of 8.4 GHz and the microwave absorption properties improved in the 9–12 GHz frequency range.

As can be seen in Figure 7 and Figure 9, the results indicate that the microwave absorbing properties of nanofiber and film samples can be improved with increasing MWNT content. Essentially, materials with high permeability can be considered as a perfect microwave absorber when they present certain value of conductivity.³⁶ MWNT has moderate magnetization and when the MWNT content in the composite structures is increased, interaction between MWNT particles leads to additional magnetic influence and higher anisotropy or eddy current which causes improving microwave absorption properties.^{25,35} In fact, four main factors contribute dielectric behavior of materials consisting of electronic, ionic, orientation and space charge polarizations. On the other hand, heterogeneity (or inhomogeneity) of the materials has an important influence on the space-charge contribution. High heterogeneity can be reached by using a large amount of MWNT leading to the more disordered motion of charge carriers and resulting in higher space charge relaxation, dipole rotation and hopping of confined charges.³⁴ The electric and magnetic energy can be dissipated with PANI and MWNT, respectively and consequently microwave absorption of PANI/MWNT samples

significantly enhance which clearly confirmed by presented graphs.

As it can be seen in both reflection loss graphs in Figure 7 and Figure 9, the position of maximum reflection loss almost remained unchanged around the frequency of 8.5 GHz at both graphs with the exception of PANIMWNT-2 sample. The following Equation can be deduced according to eq. (2), which expresses the qualitative relations among the thickness, permittivity, permeability and peak frequency.³⁷

$$f \propto \frac{C}{2\pi d \sqrt{\mu_r \cdot \varepsilon_r}} \quad (4)$$

where f is the peak frequency, d is the absorber thickness, C is the speed of the light, μ_r and ε_r are the relative complex permeability and permittivity of absorber, respectively.

The eq. (4) indicates that peak frequency is inversely proportional to thickness, relative complex permeability and permittivity of the absorber. The relation between f and μ_r , and ε_r can be investigated through fixing absorber thickness. Therefore, the peak frequency is expected to shifts toward lower frequency as the relative complex permeability and permittivity increases. Increasing in MWNT levels leads to enlarging conductivity. Since high permittivity relates to great conductivity, with increasing MWNT content from 0 to 10 wt% in samples, the relative complex permittivity raised. On the other hand, contrary to our expectation, the magnetization of absorbers might be decreased as the amount of MWNT in matrix increased which led to declining in relative complex permeability amount. The reason for this phenomenon could be predicted from promoting interfacial coupling between the carbon nanotube filler and polymer matrix which causes diamagnetic response from carbon nanotube and diminishes the total magnetization of the absorber.³⁸

According to eq. (4), considering fixed thicknesses in both nanofiber and film absorber, and this change in relative complex permittivity and permeability, remaining maximum RL peak almost unmoved is not surprising.

Comparative Results. Comparing the results of electromagnetic absorption properties of the PVA/PANI/MWNT composite nanofiber with nanocomposite film in Figure 7 and Figure 9, respectively, indicate that RL values are greatly depend on sample thickness. In fact the nanocomposite film absorbers showed higher maximum RL with -28 dB comparing to nanofiber samples with maximum RL of -23 dB. This phenomenon can be explained by dimensional resonance which increasingly enhances the microwave absorption and certainly is not related to electromagnetic properties of the material.³⁹ In order to investigating structural parameters on electromagnetic properties, nanofiber and film samples must be compared under the same thicknesses. In this work, because of fragility of the polyaniline film layer, it was impossible to prepare PVA/PANI/MWNT thin films. Therefore nanocomposite film and composite nanofiber samples were prepared in different thicknesses of 1 mm and 100 μm . Consequently,

Table I. Comparison between Relative Microwave Absorption of Composite Nanofibers Layers and Nanocomposite Films

| Material | Structure Forms | Thickness (mm) | Frequency (GHz) | RL (dB) | Relative RL (dB/mm) |
|----------------|-----------------|----------------|-----------------|---------|---------------------|
| PVA:PANI (1:0) | nanofiber | 0.1 | 11.5 | 6.5 | 65 |
| PVA:PANI (1:1) | nanofiber | 0.1 | 11.5 | 10 | 100 |
| PVA:PANI (1:1) | nanofiber | 0.1 | 11.6 | 9 | 90 |
| PVA:PANI (1:2) | nanofiber | 0.1 | 8.5 | 11 | 110 |
| PANIMWNT-0 | nanofiber | 0.1 | 8.5 | 11 | 110 |
| PANIMWNT-0 | nanofiber | 0.1 | 11 | 10 | 100 |
| PANIMWNT-2 | nanofiber | 0.1 | 8.6 | 12 | 120 |
| PANIMWNT-2 | nanofiber | 0.1 | 10.6 | 11 | 110 |
| PANIMWNT-5 | nanofiber | 0.1 | 8.6 | 11 | 110 |
| PANIMWNT-5 | nanofiber | 0.1 | 10.3 | 14 | 140 |
| PANIMWNT-10 | nanofiber | 0.1 | 10.7 | 9 | 90 |
| PANIMWNT-10 | nanofiber | 0.1 | 8.6 | 23 | 230 |
| PANIMWNT-0 | film | 1 | 8.4 | 13 | 13 |
| PANIMWNT-2 | film | 1 | 8.8 | 17 | 17 |
| PANIMWNT-5 | film | 1 | 8.5 | 18 | 18 |
| PANIMWNT-10 | film | 1 | 8.4 | 28 | 28 |

to compare microwave absorption values of films and nanofiber samples, their relative reflection loss values were compared and illustrated in Table I. As it can be seen, for all films and nanofiber samples with same substances, the relative reflection loss values for nanofibers are much higher than the film samples. Furthermore, the nanofiber absorbers presented two remarkable absorbing peaks comparing one absorbing peak in nanocomposite film absorbers. The greater microwave absorption properties in nanofiber absorbers can be attributed to the higher surface area of these materials. The large specific surface area and more active atoms at the material surface lead to large interface dielectric loss enhancing the microwave absorption properties.⁶

Comparing two graphs in Figure 7 and Figure 9 indicates that the maximum RL peak has dependence on thickness which shifts to lower frequencies as the sample thickness increased. From eq. (4) it is not hard to find that peak frequency is inversely proportional to thickness, when the relative complex permeability and permittivity of the absorber is fixed. Considering that each two compared samples fabricated with same material in this work, film absorbers showed their maximum RL in lower frequency comparing to electrospun ones.

Conclusions

In the present work, the prepared composite solutions of PVA/PANI-CSA/MWNT under various MWNT contents were successfully fabricated to composite nanofiber layers

by electrospinning process and nanocomposite films up to 10 wt% concentration of MWNT. Low surface roughness and small beads in the PVA/PANI/MWNT composite nanofiber samples were observed due to high concentration of MWNT (up to 10 wt%). All nanofiber absorbers presented two absorption peaks while nanocomposite film absorbers showed only one peak in the frequency range of 8-12 GHz. Generally the microwave absorption properties of the nanofiber absorbers with maximum relative reflection loss of 230 dB were better than nanocomposite film absorbers with maximum relative reflection loss of 28 dB and both kinds of absorbers presented an increase in maximum reflection loss with increasing in MWNT content. According to obtained results nanofiber composite layers consisting PVA/PANI/MWNT are promising candidate for microwave absorbing material in the X-band.

References

- (1) P. Saini, V. Choudhary, B. P. Singh, R. B. Mathur, and S. K. Dhawan, *Mater. Chem. Phys.*, **113**, 919 (2009).
- (2) M. S. Han, Y. K. Lee, W. N. Ki, H. S. Lee, J. S. Joo, M. Park, H. J. Lee, and C. R. Park, *Macromol. Res.*, **17**, 863 (2009).
- (3) C. J. Li, B. Wang, and J. N. Wang, *J. Magn. Magn. Mater.*, **324**, 1305 (2012).
- (4) A. Ghasemi, A. Hossienpour, A. Morisako, A. Saatchi, and M. Salehi, *J. Magnetism. Magnetic. Mater.*, **302**, 429 (2006).
- (5) Y. K. Sung and F. Tantawy, *Macromol. Res.*, **10**, 345 (2002).
- (6) D. R. J. White, *A Handbook on Shielding Design Methodology and Procedures* Gainesville, VA: Interference Control Tech-

- nologies, New York, 1986.
- (7) B. D. Che, L. T. Nguyen, B. Q. Nguyen, H. T. Nguyen, T. V. Le, and N. H. Nguyen, *Macromol. Res.*, **22**, 1221 (2014).
 - (8) Z. Wang, H. Bi, J. Liu, T. Sun, and X. Wu, *J. Magnetism. Magnetic. Mater.*, **320**, 2139 (2008).
 - (9) P. S. Neelakanta, *Handbook of Electromagnetic Materials: Monolithic and Composite Versions and Their Applications*, CRC Press, New York, 1995.
 - (10) A. G. MacDiarmid, *Synth. Met.*, **125**, 11 (2001).
 - (11) J. D. Sudha, S. Sivakala, R. Prasanth, V. L. Reena, and P. R. Nair, *Compos. Sci. Technol.*, **69**, 358 (2009).
 - (12) R. K. Paul and C. K. S. Pillai, *Synth. Met.*, **27**, 114 (2000).
 - (13) M. A. Abshinova, N. E. Kazantseva, P. Saha, I. Sapurina, J. Kovarova, and J. Stejskal, *Polym. Degrad. Stab.*, **93**, 1826 (2008).
 - (14) S. Bhadra, D. Khastgir, N. K. Singha, and J. H. Lee, *Prog. Polym. Sci.*, **34**, 783 (2009).
 - (15) T. H. Hsieh, K. S. Ho, C. H. Huang, Y. Z. Wang, and Z. L. Chen, *Synth. Met.*, **156**, 1355 (2006).
 - (16) X. Jing, Y. Wang, and B. Zhang, *Appl. Polym. Sci.*, **98**, 2149 (2005).
 - (17) N. H. Hoang, J. L. Wojkiewicz, J. L. Miane, and R. S. Biscarro, *Polym. Adv. Technol.*, **18**, 257 (2007).
 - (18) P. Saini, V. Choudhary, B. P. Singh, R. B. Mathur, and S. K. Dhawan, *Synth. Met.*, **161**, 1522 (2011).
 - (19) S. W. Phang, M. Tadokoro, J. Watanab, and N. Kuramoto, *Synth. Met.*, **158**, 251 (2008).
 - (20) J. M. Thomassin, I. Huynen, R. Jerome, and C. Detrembleur, *Polymer*, **51**, 115 (2010).
 - (21) J. E. Fischer, H. Dai, A. Thess, R. Lee, N. M. Hanjani, D. L. Dehaas, and R. E. Smalley, *Phys. Rev. B*, **55**, 921 (1997).
 - (22) K. Saeed, S. Y. Park, S. Haider, and J. B. Baek, *Nanoscale Res. Lett.*, **4**, 39 (2009).
 - (23) D. H. Park, Y. K. Lee, S. S. Park, C. S. Lee, S. H. Kim, and W. N. Kim, *Macromol. Res.*, **21**, 905 (2013).
 - (24) S. Fan, M. G. Chapline, N. R. Franklin, and T. W. Tombler, *Science*, **283**, 512 (1999).
 - (25) H. Dai, J. H. Hafner, A. G. Rinzler, D. T. Colbert, and R. E. Smalley, *Nature*, **384**, 147 (1996).
 - (26) G. Salimbeygi, K. Nasouri, A. M. Shoushtari, R. Malek, and F. Mazaheri, *Micro Nano Lett.*, **8**, 455 (2013).
 - (27) F. Raeesi, M. Nouri, and A. K. Haghi, *ePolymer*, **114**, 1 (2009).
 - (28) P. Heikkila and A. Harlin, *Eur. Polym. J.*, **44**, 3067 (2008).
 - (29) K. Desai and C. Sung, *NSTI-Nanotech*, **3**, 429 (2004).
 - (30) P. Supaphol and S. Chuangchote, *Appl. Polym. Sci.*, **108**, 969 (2008).
 - (31) E. J. Ra, K. H. An, K. K. Kim, S. Y. Jeong, and Y. H. Lee, *Chem. Phys. Lett.*, **413**, 188 (2005).
 - (32) S. B. Ni, X. H. Wang, G. Zhou, F. Yang, J. M. Wang, and D. Y. He, *J. Alloys Compd.*, **489**, 252 (2010).
 - (33) Y. Wang, Y. Huang, Q. Wang, Q. He, and L. Chen, *Appl. Surf. Sci.*, **259**, 486 (2012).
 - (34) H. S. Nalwa, *Handbook of Organic Conductive Molecules and Polymers*, John Wiley and Sons Ltd., Chichester, 1997.
 - (35) C. Y. Lee, H. G. Song, K. S. Jang, E. J. Oh, A. J. Epstein, and J. Joo, *Synth. Met.*, **102**, 1346 (1999).
 - (36) A. Kaynak, A. Polat, and U. Yilmazar, *Mater. Res. Bull.*, **31**, 845 (1996).
 - (37) Y. Feng and T. Qiu, *J. Magn. Magn. Mater.*, **324**, 2528 (2012).
 - (38) K. J. Sun, R. A. Wincheski, and C. Park, *J. Appl. Phys.* **103**, 023908 (2008).
 - (39) A. Drmota, J. Koselj, M. Drogenik, and A. Znidarsic, *J. Magn. Magn. Mater.*, **324**, 1225 (2012).